Article

Journal of Vibration and Control
19(15) 2255–2269

DOI: 10.1177/1077546313501537
jvc.sagepub.com

Harvesting energy from vibrations of the underlying structure

Bo Han[1,2], Spyridon Vassilaras[2], Constantinos B Papadias[2], Rohan Soman[3], Marios A Kyriakides[3], Toula Onoufriou[3], Rasmus H Nielsen[1] and Ramjee Prasad[1]

Abstract

The use of wireless sensors for structural health monitoring offers several advantages such as small size, easy installation and minimal intervention on existing structures. However the most significant concern about such wireless sensors is the lifetime of the system, which depends heavily on the type of power supply. No matter how energy efficient the operation of a battery operated sensor is, the energy of the battery will be exhausted at some point. In order to achieve a virtually unlimited lifetime, the sensor node should be able to recharge its battery in an easy way. Energy harvesting emerges as a technique that can harvest energy from the surrounding environment. Among all possible energy harvesting solutions, kinetic energy harvesting seems to be the most convenient, especially for sensors placed on structures that experience regular vibrations. Such micro-vibrations can be harmful to the long-term structural health of a building or bridge, but at the same time they can be exploited as a power source to power the wireless sensors that are monitoring this structural health. This paper presents a new energy harvesting method based on a vibration driven electromagnetic harvester. By using an improved Maximum Power Point Tracking technique on the conversion circuit, the proposed method is shown to maximize the conversion coefficient from kinetic energy to applicable electrical energy.

Keywords

Energy harvesting, maximum power point tracking, micro generator, structural health monitoring

1. Introduction

Vibrations of manmade structures such as buildings, bridges, railway lines and roads can be very harmful for their structural safety in the long term. For instance, such vibrations can cause inner force imbalance, cracks inside the structures, or instability/unreliability of the riveting point (Beeby et al., 2006). Vibrations in certain low harmonic frequencies can even cause resonance of the structure that can lead to disastrous consequences such as partial or complete collapse. Structural health monitoring (SHM) is adopted as a method that can detect micro-changes inside the structure thus assisting preventive maintenance and issuing alerts for repairs to be conducted ahead of the breakpoint (En et al., 2010). The easiest way to install such an SHM system is to integrate a grid of wired sensors inside the structure during construction. However, for most of the existing infrastructures it is not a good solution to open holes or run wires to install this type of equipment as this might damage the structure itself or adversely affect its aesthetics and functionality (Lynch and Loh, 2006). Furthermore, integrated wired sensors suffer from a number of other limitations such as lack of flexibility to make configuration changes, damaged cabling repairs and hardware upgrades.

A solution to the aforementioned concerns is to use a wireless sensor network (WSN) for SHM. A WSN consists of a number of small sensing devices (called sensors or WSN nodes) which send the monitored data to a fusion center wirelessly and can be easily installed on the surface of the infrastructure without

[1]CTiF, Electronic Systems, Aalborg University, Aalborg, Denmark
[2]Athens Information Technology, Athens, Greece
[3]Cyprus University of Technology, Limassol, Cyprus

Received: 15 July 2013; accepted: 17 July 2013

Corresponding author:
Bo Han, Aalborg University, Aalborg, Denmark; Athens Information Technology, 0.8 km Markopoulou Avenue, PO Box 68, 19002, Peania, Greece.
Email: hab@es.aau.dk

inflicting further damage. For this reason, WSNs are widely used in SHM (Lynch and Loh, 2006). One of the main challenges in WSNs is power consumption. Sensors are commonly powered by batteries, which need to be replaced by human personnel when they get depleted (Han et al., 2012). Since this is not always easy to do, the energy lifetime of sensors' batteries and thus the frequency of required battery replacements becomes a big concern. There are two ways to extend battery lifetime. One way is by reducing the power consumption of sensors (by designing energy efficient hardware and software) and the other way is by powering the nodes with self-rechargeable batteries capable of harvesting energy from the surrounding environment (Sazonov et al., 2009). See Casciati and Rossi (2007) for a detailed discussion on the various types of rechargeable batteries and large capacitors that can be used to store harvested energy.

There are many forms of energy that can be converted to electric energy, such as:

- Solar energy, which can be converted to electric energy by photovoltaic solar cells, but depends on the availability of sunlight at the exact place where the sensor is placed;
- Electromagnetic energy (RF waves), which can be converted to electric energy by electromagnetic energy converters (used for example in long-range RFIDs), but suffers from signal path loss;
- Thermal energy, which can be converted to electric energy by thermal energy converters that generate current in the circuit from thermal difference on electro probes, but needs large enough thermal differences; and
- Kinetic energy which will be extensively analyzed in this paper.

The most popular methods of energy harvesting and their corresponding power densities and limitations are summarized in Table 1, which shows that solar energy harvesting offers the highest power density while thermal energy harvesting comes second. However, in applications where there is not enough sunshine or big thermal differences and the sensors are placed in an environment rich in vibrations, the most convenient way of harvesting energy is to convert the kinetic energy of such vibrations to electric energy. For example in SHM applications where sensors are meant to monitor vibrations and their effects on structures, harvesting the energy of such vibrations comes as a natural choice (Halvorsen, 2008).

Table 1. Comparison of energy harvesting techniques.

Type	Power density (W/cm^2)	Limitations
Solar	20 μ-200 m	Light intensity
Thermal	30 μ-30 m	Thermal difference
RF wave	200 p-1 m	Distance and RF harmonic
Vibration/PZT	4 μ-200 μ	Vibration frequency
Vibration/EM	25 μ-10 m	AC/DC conversion

It is also clear from Table 1 that electromagnetic (EM) based kinetic energy harvesting has much higher power density than piezoelectric (PZT) energy harvesting. Moreover, as pointed out in Casciati and Rossi (2007) in civil engineering applications, natural vibration frequencies of structures fall in the range 1–100 Hz, which is about an order of magnitude lower than what is required for an efficient PZT energy harvester. Therefore an electromagnetic based micro-generator is the preferred method for vibration energy harvesting (Kulkarni et al., 2008).

In order to maximize the energy output, the energy harvester needs to be placed at the point where the maximum vibration amplitude is attained (Kulkarni et al., 2008). The use of an appropriate vibration model for the structure to be monitored can provide an insight on the maximum kinetic energy as well as the energy distribution on the vibrating object. In this paper we are considering vibration models of a bridge and calculate the vibration energy that can be harvested at various points on the bridge. We are also proposing certain optimizations to the micro-generator for energy harvesting, in order to achieve maximum conversion to electrical power. Another issue with EM energy conversion (as shown in Table 1) is that it generates a very weak alternating current (AC) voltage whereas most sensors operate at direct current (DC) voltage. A nice overview of power and supply voltage requirements for sensors used for SHM can be found in Casciati et al. (2012). To address this issue, we propose a simple rectifier circuit (based on a Maximum Power Point Tracking (MPPT) technique) which can efficiently convert the EM harvester output from a weak AC voltage to a higher DC voltage for the follow-up circuits.

Energy harvesting of micro-vibrations has received considerable attention recently in the scientific literature. A number of different approaches have been proposed for amplifying the very low voltage produced by micro-generators and rectifying the low frequency AC voltage into DC voltage required for follow-up sensor circuitry. Cheng et al. (2011) provide a nice literature overview of the various approaches and discuss the respective advantages and limitations of each approach.

A broad categorization of approaches is whether they are based on active circuit components (requiring an external power source) or completely passive circuit

components. In the first case the circuit output needs to be used to power these active components as well as the follow-up circuit. This creates the need for a bootstrapping phase in which an external power source (e.g., a battery) is typically needed. Passive circuit designs, on the other hand, are usually combined with a transformer (to amplify the input AC voltage) which is of considerable size and cannot be integrated in a compact circuit. In addition such a transformer implies an increased load burden for the harvester.

The same paper (Cheng et al., 2011) goes on to propose an active circuit voltage multiplier-based technique that can convert input voltage ranging from 0.35 V to 2 V and 20–500 Hz to a DC output voltage with a gain factor of 8. The proposed circuit design is based on active diodes which can eliminate the threshold voltage problem of traditional passive diodes. However, the circuit topology is based on the conventional voltage stack multiplier which cannot optimally adapt to the power requirements of the follow-up circuit.

A most recent example of a passive circuit approach is that of McCullagh et al. (2012), which also proposed a parametric frequency increased generator that can convert the low vibration frequency of the bridge to higher frequency mechanical oscillations of the harvester mass, in order to increase harvester performance. As the employed voltage boosting technique is the conventional diode-capacitor stack multiplier, which has the limitation on the threshold voltage of the first stage, the authors introduced a 1:10 transformer connected between the harvester and the voltage rectifier.

A hybrid technique, which uses passive circuit components at the first stage and the output of this first stage to power the active circuit components of the second stage, is introduced in Ulusan et al. (2012). This second stage circuit also uses actives diodes which can be fabricated using CMOS technology to achieve better integration and compact size. However, a three-stage amplifier was proposed to be used as a comparator, which increases circuit complexity and reduces reliability. More importantly, the voltage gain achieved by the proposed rectifier circuit is small (about 2x) as it can provide an output voltage of 1.8 V at a 1 V input voltage.

In this paper, we introduce an electromagnetic energy harvester using a simple, active voltage-rectifier circuit based on the maximum power tracking technique. The proposed circuit can adjust the total load seen at the output of the electromagnetic micro-generator in order to achieve maximum energy conversion efficiency. In addition, rather than considering only the mechanical domain or the electrical domain, we consider the mechanical and electrical damping jointly in order to maximize the harvested energy. Finally, in this paper we present both the mechanical/civil engineering background and an electrical circuit technique for energy harvesting using electromagnetic micro-generators.

The rest of the paper is organized as follows. Section 2 gives the system description and introduces a detailed vibration model for a bridge, including the vibration function of the energy harvester. Section 3 provides an analysis of the electromagnetic micro-generator. The follow-up conversion circuit for voltage regulation and power extraction is developed in Section 4. Simulation results are presented in Section 5. Finally, the main conclusions of this study are given in Section 6.

2. Vibration model

2.1. Vibration of the underlying structure

The response of a bridge under a moving load, P, can be described by equation (1) (Fryba et al., 1999; Stancioiu et al., 2011)

$$m\frac{\partial^2}{\partial t^2}y(x,t) + c\frac{\partial}{\partial t}y(x,t) + EI\frac{\partial^4}{\partial x^4}y(x,t) = \delta(x-vt)P \tag{1}$$

where $y(x,t)$ is the vertical displacement of the bridge at position x along the bridge and at time t, m is the mass per unit length of the bridge, L is the length of the bridge, c is the damping coefficient, E is the Young's Modulus of the structure, I is the second moment of area, P is the force applied as a result of the moving load, and v is the magnitude of the velocity of the moving load along the x direction (Ali et al., 2011). The Dirac-delta function on the right side of the equation physically represents the point load that is applied on the bridge while it moves along the bridge. In reality, the bridge is subjected to multiple loads due to several vehicles at a time. The effect of multiple loads can be obtained by superposition of the response to individual loads. This superposition is possible due to the linear response of the bridge structure.

The solution of the partial differential equation equation (1) has the general form

$$y(x,t) = \sum_{j=1}^{M} \phi_j(x) q_j(t) \tag{2}$$

where $\varphi_j(x)$ is the j^{th} mode shape function of the bridge, $q_j(t)$ is the j^{th} modal displacement, and M is the number of modes of significance, as the contribution of the higher modes is negligible.

The mode shapes $\varphi_j(x)$ in the generalized solution of the partial differential equation are independent of time t, and satisfy the boundary conditions, while $q_j(t)$ are independent of the spatial co-ordinate x and satisfy the initial conditions (Li et al., 2008).

Equation 2 can be written in the frequency domain as follows

$$Y(x,\omega) = \sum_{j=1}^{M} \varphi_j(x) Q_j(\omega) \tag{3}$$

where $Q_j(\omega)$ is the j^{th} modal displacement in the frequency domain (Yang et al., 2004).

The natural frequencies and mode shapes of the bridge depend on the sectional properties of the bridge and its boundary conditions. Thus, knowing the modal properties of the structure, end conditions and the excitation due to the moving load, the response of the structure can be simulated.

2.2. Bridge description

To validate the methodology, a numerical model of the Grand-Mere Bridge, in Quebec, Canada, a typical medium span bridge (Figure 1) was used. The bridge is a single-cell box-girder type bridge with three continuous spans of 40 m, 181 m, and 40 m, with a wedge shaped cantilever of 12 m at either end. The 40 -m spans on either side have a linearly changing cross section. For the central span the depth varies in a parabolic manner.

The wedge shaped cantilevers are of solid cross section increasing to a depth of 8.53 m at the external piers. The compressive strength of concrete in mid span is 38 MPa, while compressive strength of the concrete at the end spans is 34 MPa. The bridge has hinged supports at the ends and is simply supported at the internal piers and external piers. More details on this bridge can be found in Massicotte et al. (1994).

2.3. Bridge modeling

The commercial finite element software ABAQUS (version 6.11ed, 2011) was used to simulate the response of the Grand-Mere Bridge under a moving load and extract the significant mode shapes. The girder was modeled using beam elements each of 1 m in length. The section properties for the elements were computed using the data available in Massicotte et al. (1994).

The moving load was assumed to be a three-axle HS20 truck (Cantero et al., 2009) as this corresponds to 65% of the traffic observed on middle span bridges based on Weigh in Motion (WIM) data

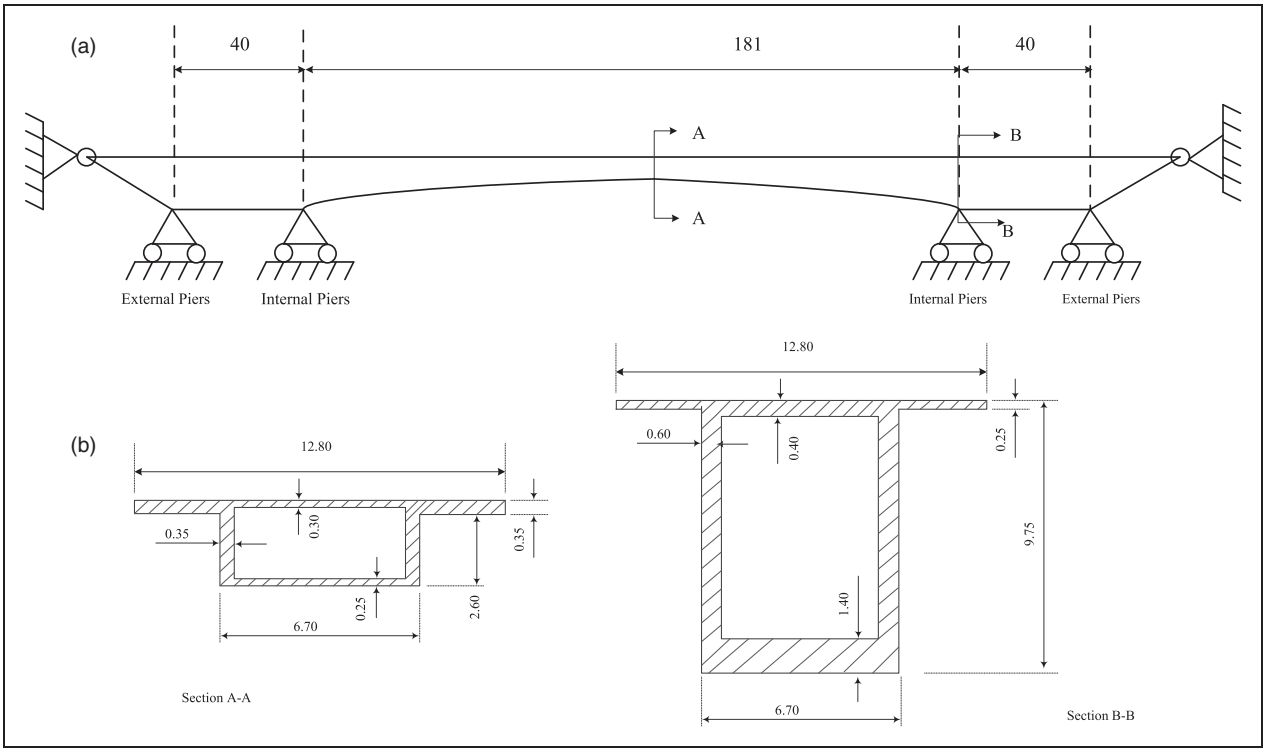

Figure 1. Details of Grand-Mere Bridge, all dimensions are in meters (m). (a) Schematic of Grand-Mere Bridge (longitudinal view); (b) cross-section of the bridge at the piers and mid span.

(Jacob and Labry, 2002). Based on statistical analysis Cantero et al. (2009) showed that the average load of a loaded HS20 truck is 600 kN and the load distribution over the three axles can be assumed to be 1:2:2. Thus, the loading scenario for the bridge was simulated as three point loads at a fixed distance apart moving at a constant velocity along the bridge.

2.4. Harvester dynamics

The energy harvester is considered as a single-degree-of-freedom (s-d.f.) system, which means that the harvester will move at the same direction of the bridge vibration described by $y(x, t)$ (Sun, 2001). The harvester is subjected to a forced vibration as a result of the

bridge response to the moving load described in the previous section (Ali and Ramaswamy, 2009).

Figure 2 gives the conceptual model of the energy harvester, where a moving mass is fixed to the vibration base with a spring and two dampers (Carrella et al., 2009). The mass of the harvester is given by M_H, the mechanical damping factor is given by ξ_m , the electrical damping factor is given by ξ_e, the stiffness of the spring is denoted by k_p, the acceleration of the vibration base (external excitation) is given by $\partial^2 y(x, t)/\partial t^2$, and the movement of the mass inside the harvester is given by y_2. Thus the vibration function of the energy harvester is given by Carrella et al. (2009).

$$M_H \frac{\partial^2 y_2}{\partial t^2} + \xi_m \frac{\partial y_2}{\partial t} + \xi_e \frac{\partial y_2}{\partial t} + k_p y_2 = -M_H \frac{\partial^2 y(x,t)}{\partial t^2} \quad (4)$$

This equation is a general equation for all kinds of vibration-based energy harvesters; it can be either a piezoelectric energy harvester or an electromagnetic energy harvester. Note that the external excitation of the harvester mass in the right hand side of equation (4) is obtained by solving equation (1). It should also be noted that when calculating the energy harvester vibration equations, we can consider the acceleration of the vibration base $\partial^2 y(x, t)/\partial t^2$ as constant when $\partial^2 y_2/\partial t^2$ is calculated. The total energy that is harvested from the energy harvester is given by Elvin et al. (2006).

$$E = \int_0^t \xi_e \left(\frac{\partial y_2}{\partial t}\right)^2 dt \quad (5)$$

The electrical damping factor ξ_e depends on the electrical circuit driven by the micro-generator. The following equation links the mechanical (velocity of the moving mass) and electrical (output voltage) quantities of the micro-generator

$$\Theta V + \xi_e \frac{\partial y_2}{\partial t} = 0 \quad (6)$$

where Θ is the coefficient of mechanical-electrical coupling, and V is the associated output voltage of the energy harvester. Substituting (6) into the vibration equation of the energy harvester (4), we have

$$M_H \frac{\partial^2 y_2}{\partial t^2} + \xi_m \frac{\partial y_2}{\partial t} - \Theta V + k_p y_2 = -M_H \frac{\partial^2 y(x,t)}{\partial t^2} \quad (7)$$

For a piezoelectric-material-based energy harvester, the electrical equation can be expressed as

$$\Theta \frac{\partial y_2}{\partial t} + C \frac{\partial V}{\partial t} = i \quad (8)$$

where i is assumed to be the output current, and C is the piezoelectric capacitance.

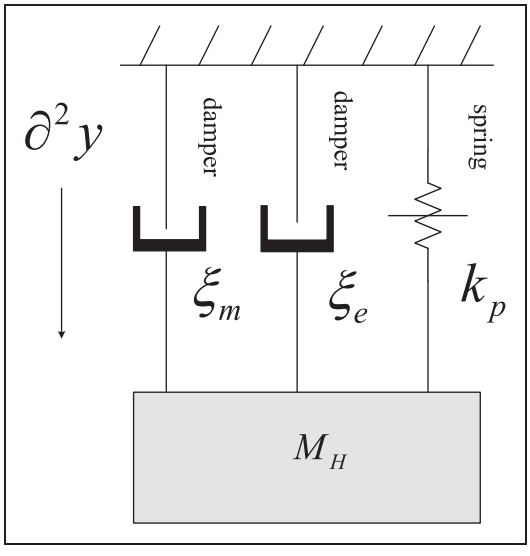

Figure 2. Generic vibration harvester conceptual model.

3. Electromagnetic energy harvester

3.1. Electromagnetic micro-generator

The magnetic-based energy harvester can be implemented in many configurations. The simplest model uses a static permanent magnet with one vibration coil, as shown in Figure 3 (a).

The basic depiction of components in the electromagnetic harvester is given in Figure 3(a), where the bottom is attached to the bridge. As the vibration $y(x, t)$ induced force, f is applied to the entire harvester the mass, M, vibrates inside the coil. Such a mechanism can be modeled as a wire coil attached to a seismic mass. An electrical current is generated at the coil when the iron mass oscillates inside the magnetic field

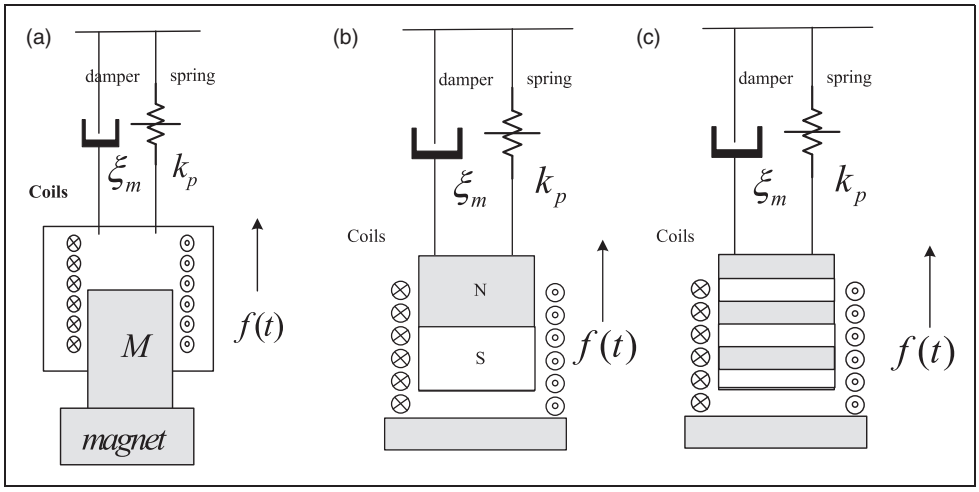

Figure 3. Electromagnetic vibration harvester configurations.

created by the magnet. Due to the magnetic flux changes inside the coil, an induced current will flow in the coil, which can be used to power the load. The current will go through the load in a closed circuit loop. In this way the coil is considered as a micro electrical generator (Han et al., 2013).

Let us denote the displacement of the mass inside the coil byy_2, the oscillating mass by M_H and the force driving the permanent magnet by $f(t)$ (Figure 3 (a)). This force is caused by the bridge vibration acceleration$\partial^2 y(x,t)/\partial t^2$. Thus the vibration equation of such an electromagnetic-based energy harvesting system is given by equation (4).

The total amount of energy harvested by the harvester depends heavily on the configuration parameters of the harvester, such as the number of turns of the coil, N, the topology of the permanent magnetic placement (Figure 3 (b) and (c)), the vibration frequency,ω, and the amplitude of the displacement, y_2 , which is influenced by the acceleration, $\partial^2 y(x,t)/\partial t^2$, of the base vibration. Improved magnetic energy harvester configurations are shown in Figure 3, where the coil is static while the vibrating mass consists of two magnetic poles (Figure 3 (b)) or a multiple poles magnetic stack (Figure 3 (c)). In this kind of configuration, each displacement will cause two or N times the magnetic flux change obtained in Figure 3 (a). Assuming Φ is the magnetic flux inside each coil turn of the harvester, the output voltage of such an EM energy harvesting system is given by

$$V_i = KN\frac{\partial \Phi}{\partial t} = KN\frac{\partial \Phi}{\partial y_2}\frac{\partial y_2}{\partial t} = KN\frac{\partial \Phi}{\partial y_2}y_2' \tag{9}$$

where, K, is the number of magnetic stacks, and y_2 is the displacement of the vibrating magnet. Assuming a load with impedance $Z_{Load} = R + jX_{c,l}(\omega)$ is connected to the energy harvester, the current is given by $i = V_i/Z_{Load}$. The total energy harvested in a time interval [0, t] can be expressed as

$$\begin{aligned} E_{em} &= \int_0^t V_i \cdot i \, dt = \int_0^t \left(\frac{KN}{Z_{load}}\frac{\partial \Phi}{\partial y_2}\frac{\partial y_2}{\partial t}\right)^2 Z_{load} dt \\ &= \int_0^t \left(\frac{KN}{Z_{load}}\frac{\partial \Phi}{\partial y_2}\right)^2 Z_{load}\left(\frac{\partial y_2}{\partial t}\right)^2 dt \end{aligned} \tag{10}$$

Such energy can be considered as being generated by an equivalent (conceptual) electrical forceF_{ed}, so that the energy generated from such equivalent force can be written as $W = F_{ed} \cdot y_2$, following the classical physics equation for work. By equating this virtual energy with the actual converted electrical energyE_{em}, we obtain the following expression for the electrical force F_{ed} :

$$F_{ed}dy_2 = V \cdot idt \Rightarrow F_{ed} = \frac{V \cdot i}{\partial y_2/\partial t} \text{ or } F_{ed} = KN\frac{\partial \Phi}{\partial y_2} \cdot i \tag{11}$$

Note that each term in equation (4) represents a force. Thus the electrical force F_{ed} is given in terms of the electrical damping factor as $F_{ed} = \xi_e \frac{\partial y_2}{\partial t}$. Therefore the electrical damping factor depends on the load of the attached electrical circuit and the characteristics of the micro-generator as follows:

$$\begin{aligned} \xi_e &= \frac{F_{ed}}{\partial y_2/\partial t} = \frac{KN}{\partial y_2/\partial t}\frac{\partial \Phi}{\partial y_2} \cdot i = \frac{KN}{\partial y_2/\partial t}\frac{\partial \Phi}{\partial y_2} \cdot KN\frac{\partial \Phi}{\partial y_2}\frac{\partial y_2}{\partial t}/Z_{load} \\ &= \left(KN\frac{\partial \Phi}{\partial y_2}\right)^2/Z_{load} \end{aligned} \tag{12}$$

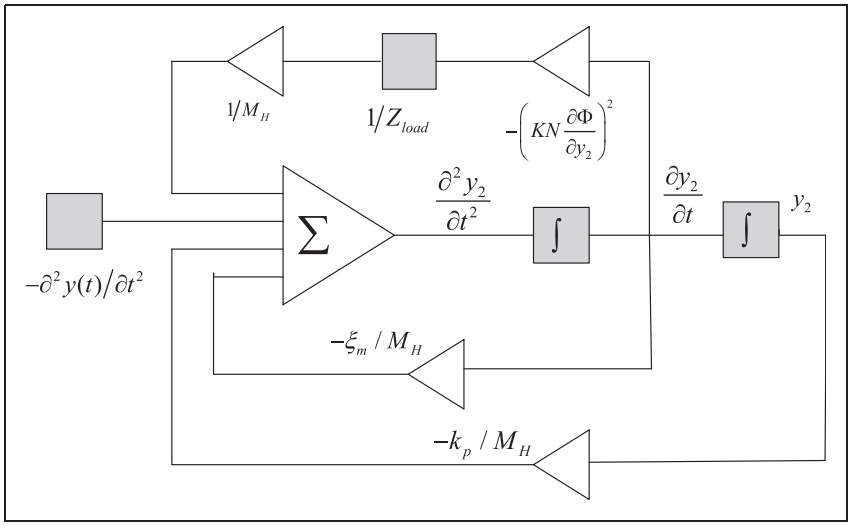

Figure 4. Electrical model of the energy harvester.

3.2. Equivalent model in the electrical domain

The proposed energy harvester is modeled as shown in Figure 4, which gives a schematic illustration of the numerical effective electrical model of the energy harvester that converts energy from the mechanical to the electrical domain. The small triangles stand for the different coefficients from various domains and the square rectangle on the main chain stands for the derivation or integration of the main function in the loop. The

external source is denoted by the left square rectangle which is assumed to be the external mechanical vibration from the bridge. The entire energy harvester is considered as a limited feedback system with external input.

An alternative representation of the harvested energy in terms of the total available kinetic energy is as follows. Assuming that the number of vibration modes of significance is J, the mechanical energy propagation efficiency from the vibrating bridge to the vibrating mass in the micro-generator is η_j, and the conversion efficiency from mechanical energy of the vibrating mass to the harvested electric energy is λ_j, the total output energy for the energy harvester is given by equation (13):

$$E_{eh} = \sum_{j=1}^{J} \eta_j \lambda_j E_m^j \tag{13}$$

where E_m^j is the mechanical energy of the j^{th} vibration mode at the point of sensor placement calculated from the vibration model of the bridge. With a fixed total available kinetic energy E_m, the maximum electrical power has an optimal value. Due to the fact that different electric loads applied to the energy harvester will affect the electrical damping factor of the micro-generator, the energy conversion efficiency is dependent on the follow-up circuit to be powered by the harvester. Note that the mechanical energy propagation efficiency η_j depends on the natural frequency of the vibrating mass. For maximum efficiency, this natural frequency should be matched with one of the frequency modes of the bridge at the point where the micro-generator is placed. This is a limitation of the EM micro-generator as a suitable micro-generator should be built according to its point of placement.

Recall that the vibration equation with mechanical damping and electrical damping is equation (4), where the vibration function contains a mechanical damping factor, ξ_m , and also an electrical damping factor, ξ_e. The electrical damping can be physically explained as it is caused by the load connected to the energy harvester, e.g., a big electrical load will exert additional damping for the energy harvester which will make the internal magnetic core more difficult to move. Thus, the load after the energy harvester will influence the effective electrical damping of the harvester which is considered as an additional ''burden'' for the energy converter. In most cases, the load connected to the energy harvester is considered to be a complex number, which means the load is not only a pure resistive load, but also has an energy storage component, which is given by

$$Z_{Load} = R + jX_{c,l}(\omega) \tag{14}$$

where R is the pure resistive load and $X(\omega)$ is the imaginary load. For the operation of the energy harvester, since the vibration is dynamic and changing all the time, such a change in the load will alter the effective electrical damping factor of the vibration model.

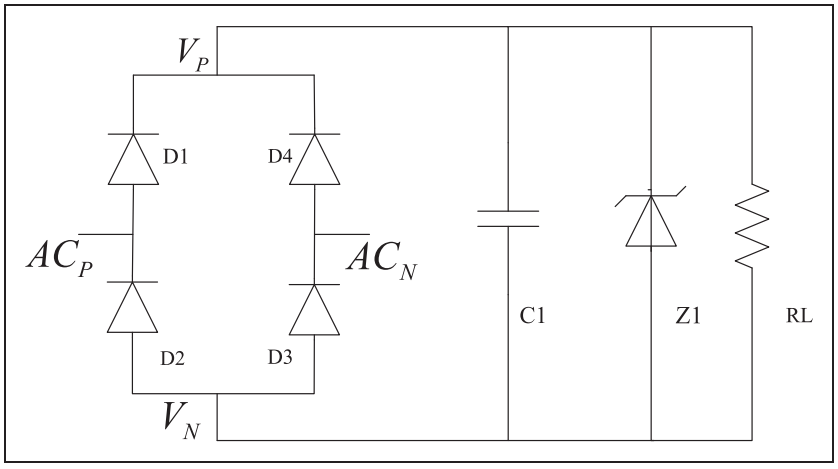

Figure 5. Conventional full bridge converter.

The inductor-based load model will also change the energy calculation function.

4. Voltage regulator

4.1. Voltage regulator analysis

As mentioned in the previous section, the electric load of the energy harvester will influence the system conversion efficiency, thus an electrical circuit stage after the harvester should be carefully chosen. Furthermore, the output voltage of the energy harvester is so weak that it cannot be used by the follow-up circuit directly. The most common way of using such harvested energy is to store it in a capacitor and discharge the capacitor to charge the battery or power up the circuit directly. In addition, due to the inherent characteristics of the electromagnetic energy harvester, the amplitude of the output voltage is time varying. Because most low power sensor nodes require a DC voltage, a regulation circuit that can do the conversion from AC to DC is also needed.

This voltage regulator is a circuit stage added between the micro-generator and the follow-up circuit. A very common voltage regulator that converts AC to DC is the ''half-bridge-switch'' and ''full-bridge-switch'' voltage regulator, which is composed by four PN diodes, from which the output current can only flow towards one direction (from VP to VN), as shown in Figure 5.

The operation of this voltage regulation is very simple. The AC voltage is applied to the points AC_P and AC_N. At the positive cycle of the input AC voltage, the PN diodes D1 and D3 are switched on, thus the current can only flow from AC_P to node V_P and from V_N to AC_N. At the negative cycle, the PN diodes D2 and D4 are switched on, and the current can only flow from V_N to AC_P, and from AC_N to V_P. Therefore, the current can only go out from V_P, and only into V_N and this results in transforming alternating current into current flowing always into the same direction (albeit with varying amplitude). With the further help of the charge storage capacitor C1, the final output voltage will be close to fixed amplitude DC voltage.

However, there are some disadvantages of the full-bridge-switch voltage rectifier. First, the threshold voltage of a PN diode which is typically 0.5–0.7 V is relatively high, and might not fall in the range of the output voltage of the micro-generator. Second, the full-bridge-switch cannot provide any voltage gain to meet the requirements of the following stages.

4.2. Rectifier with maximum power point tracking (MPPT)

Because of this problem, an improved voltage regulator with Maximum Power Point Tracking (MPPT) (Rahimi et al., 2012) technique is proposed in this paper. Unlike the conventional ''full-bridge'' voltage regulator, the rectifier shown in Figure 6 can boost voltage to a larger value. Moreover, the additional inductor L_{ad} and resistor R_{ad}, can be selected so that the total load, Z_{Load} , and consequently the electrical damping factor, ξ_e, are optimized for maximum energy efficiency (Dwari and Parsa, 2009).

The regulator circuit in Figure 6 operates as follows – the two switches M1 and M2 are based on NMOS and PMOS respectively and are turned ON or OFF simultaneously. Using two switches results in a better behavior to bidirectional current flow (current can flow through the switches either from left to right or from right to left). The two switches are turned ON when the controlling signal *pwm1* generated by the PWM generator is positive and turned OFF when it is negative (see Figure 7 [The plots in Figures 7, 8 and 9 were generated

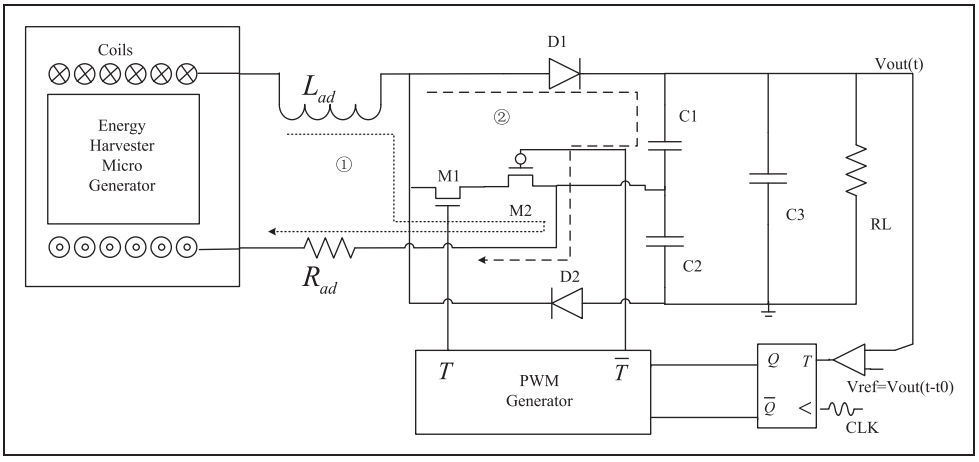

Figure 6. The adaptive Maximum Power Point Tracking circuit.

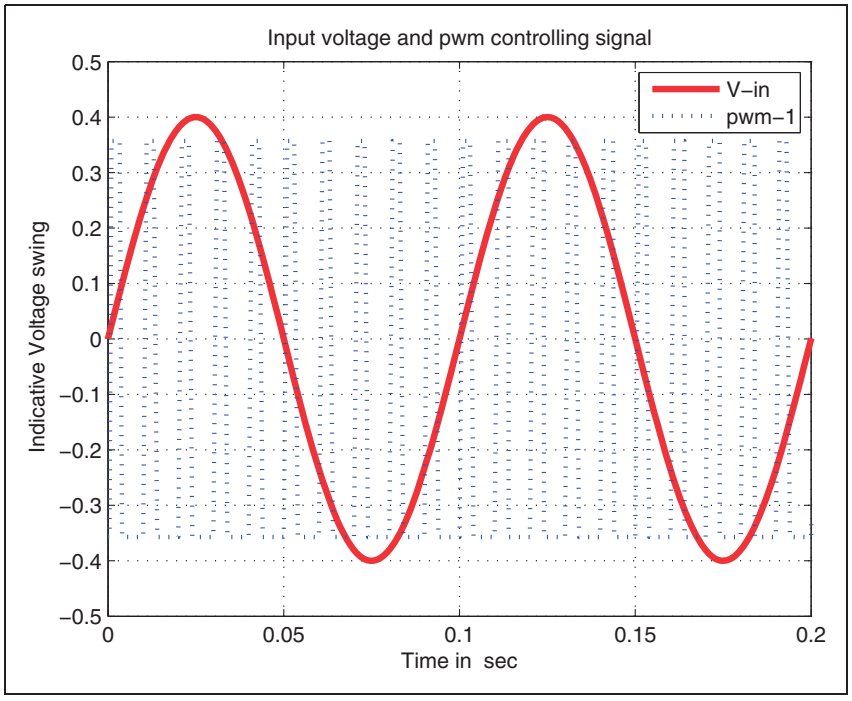

Figure 7. The controlling signal (dashed curve) and input voltage (solid curve).

by simulating the circuit in Figure 6 using the Advanced Design System (ADS) 2008 circuit simulation tool by Agilent Technologies.]).

During the positive cycle of the rectifier input voltage, when the switches M1 and M2 are turned ON by their controlling signal, the current flows as shown in Figure 6 – current path, through *L_ad*, M1, M2 and *R_ad*. After time t_1 (still during the positive cycle of the input voltage Vin as shown in Figure 7), switches M1 and M2 are turned OFF, the inductor-stored current flows together with the voltage-induced current and the aggregate current will go though D1 and charge C1 as shown in Figure 6 – current path. The switching period is much shorter than the input voltage period, and so the voltage starts accumulating.

During the negative cycle of the input voltage, a similar process will take place through the symmetric circuit consisting of D2 and C2. By adjusting the switch-on duty cycle $D = t_1/T_S$ (where t_1 is the ON time and T_S is the controlling signal period) the output voltage can reach a higher value than the input voltage (see Figure 8), which is the advantage

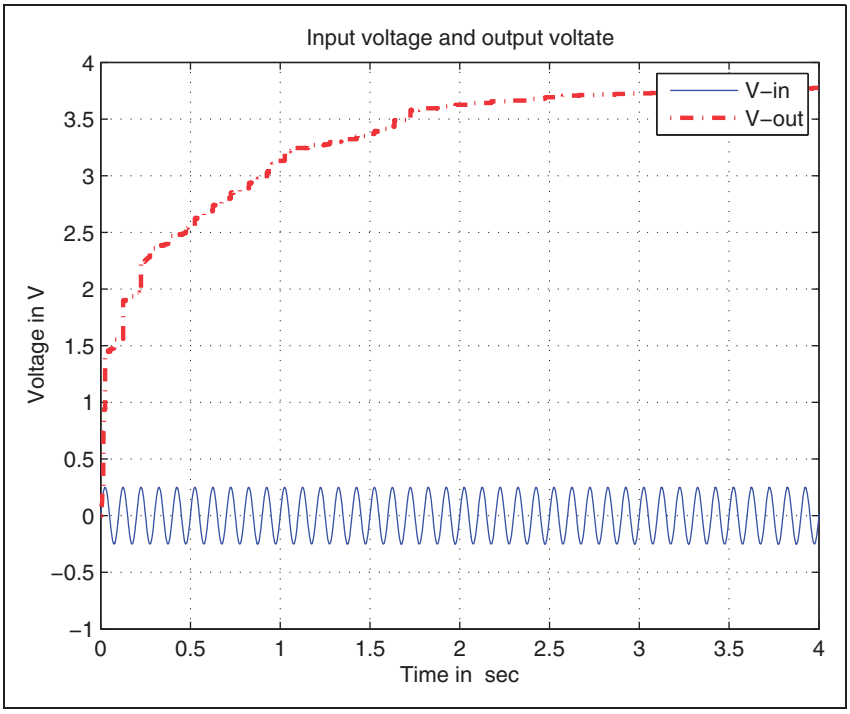

Figure 8. The input voltage (solid line) and output voltage (dashed line).

of such a voltage-boosting rectifier compared to the conventional full-bridge AC-DC rectifier. The capacitor C3 is added to further stabilize the output voltage seen by the follow-up circuit RL.

Let us now explain the functionality of the D-flip-flop and feedback loop shown in Figure 6. When the output of the proposed voltage-boosting circuit has reached the required level (typically in the range 3.3 V∼4.2 V for wireless sensors), the feedback mechanism can achieve maximum output when the follow-up electrical load (indicated by RL in Figure 6) changes. Such a change can be the result of increasing demand at the next stage's circuit, e.g., the sensor starts a wireless transmission. The feedback system can then adjust the duty cycle of the controlling signal so that the maximum energy is delivered to the load.

Detecting the demand of the circuit can be done by monitoring the current change or the voltage change; when the power demand is increasing, the current will increase and the output voltage will drop. The mechanism proposed here takes the voltage as a monitoring reference.

The reference voltage (V_{ref}) is a delayed (by t_0) version of the output voltage (V_{ref} (t) = V_{out}(t-t_0)). If $V_{ref} < V_{out}$, which means that the system consumes increasing power, the comparator will give an output voltage that triggers the PWM to increase the duty cycle so that the output voltage will be increased to satisfy the follow-up circuit requirements. But when $V_{ref} > V_{out}$, which means that the next stage's circuit is not as heavily loaded, the duty cycle will be decreased and the output voltage will be decreased until this feedback is balanced. Thus the maximum power tracking is performed in such a way that increases the conversion efficiency.

One way (among many other ways) of realizing such feedback is to let the output of the comparator go into a D-flip-flop, which produces two complementary outputs Q and $\overline{Q}$. When $V_{ref} < V_{out}$, the output of the D-flip-flop will drive the PWM generator to increase the pulse duty cycle, which results in increasing the output voltage.

Now let us denote the input voltage to the rectifier by $V_i(t)$ with peak voltage V_{ip} and period T_i, the switching period of the switches M1 and M2 by T_s with associated frequency f_s, and the output voltage of the rectifier by $V_o(t)$. As explained in Section 3, the electrical damping factor of the system is influenced by the changing load $Z_{load} = R + jX_{c,l}(\omega)$. It can be shown that by using the proposed circuit, the total load is given by the following equation

$$Z_{load}(total) = (R\_ad + R_{ef}) + j\omega L\_ad \qquad (15)$$

where R_{ef} is given by

$$R_{ef} = 2L\_ad/\beta D^2 T_s \qquad (16)$$

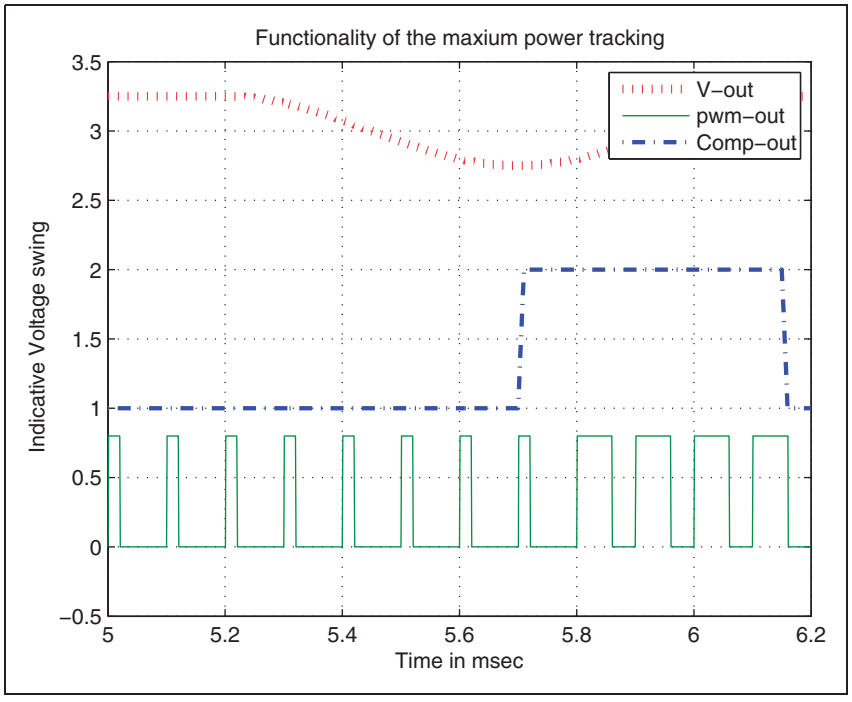

Figure 9. The output voltage can be adjusted by changing the duty cycle of the controlling signal (the output of the PWM generator and the output of the comparator are scaled and shifted in order to fit all curves in one figure).

where D is the duty cycle, T_s is the switching period, and β is given by:

$$\beta = 2\int_0^{2\pi} \sin^2\theta\left[1 - \frac{\sin\theta}{V_0/V_{ip}}\right]^{-1} \mathrm{d}\theta \tag{17}$$

where θ is given by $\theta = 2\pi t/T_i$. Therefore the total load for the harvester can be derived as

$$\begin{aligned} Z_{load}(total) &= \left(R\_ad + \frac{2L\_ad}{\beta D^2 T_s}\right) + j\omega_i L\_ad \\ &= R\_ad + j\left(\frac{4\pi\omega_s}{\beta D^2} + \omega_i\right) L\_ad \end{aligned} \tag{18}$$

Thus the total load is a complex load, and the switching frequency and input voltage frequency also influence the actual load, which will in turn influence the maximum harvestable power.

Note that the proposed regulator circuit includes active circuit components that need power supply. This implies the need for a bootstrapping phase during which external power is needed (e.g., by a battery). Once the output voltage of the circuit is high enough this can be used to power the active components of it and the external power supply is no longer needed (provided that the micro-vibrations can generate enough energy to keep the power stored at the capacitors above a required level at all times).

5. Simulated results and analysis

In this section we present simulation results based on typical mechanical parameters for the bridge model and vibration model, and suitable electromagnetic parameters for the electromagnetic-based micro-generator energy harvester, as well as circuit element parameters for the voltage regulator.

The maximum displacement (deflection) at the middle point of the bridge analyzed in Section 2 is obtained assuming a moving load with the characteristics of an HS20 truck presented in Section 2.3.

From Figure 10 we can see the deflection of the midpoint has a maximum of 1.15 mm at vehicle speed 30 m/s. The figure shows the transient characteristics of the vibration and illustrates that harvestable energy is only available when loads are moving on the bridge. The vibrating mass of the energy harvester is assumed to be $M_H = 9g$ and the mechanical damping $\xi_m = 0.038$. The turn number of the coil is assumed to be $N = 250$, the number of magnetic stacks $K = 6$ and the spring stiffness k_p in the harvester $k_p = 4.186N/mm$. Finally, the flux leakage Φ is assumed as $\partial\Phi/\partial y_2 = 12.5\mu B/mm$, and the load of the harvester has real value

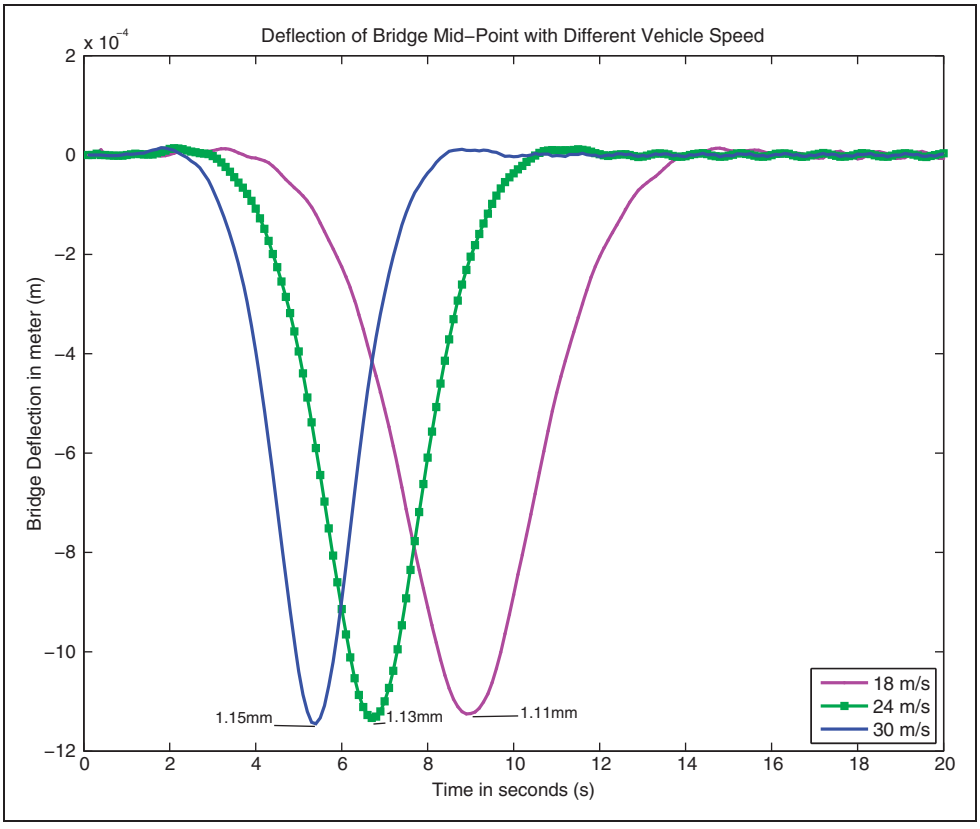

Figure 10. Maximum deflection of the mid-point of the bridge at different velocities.

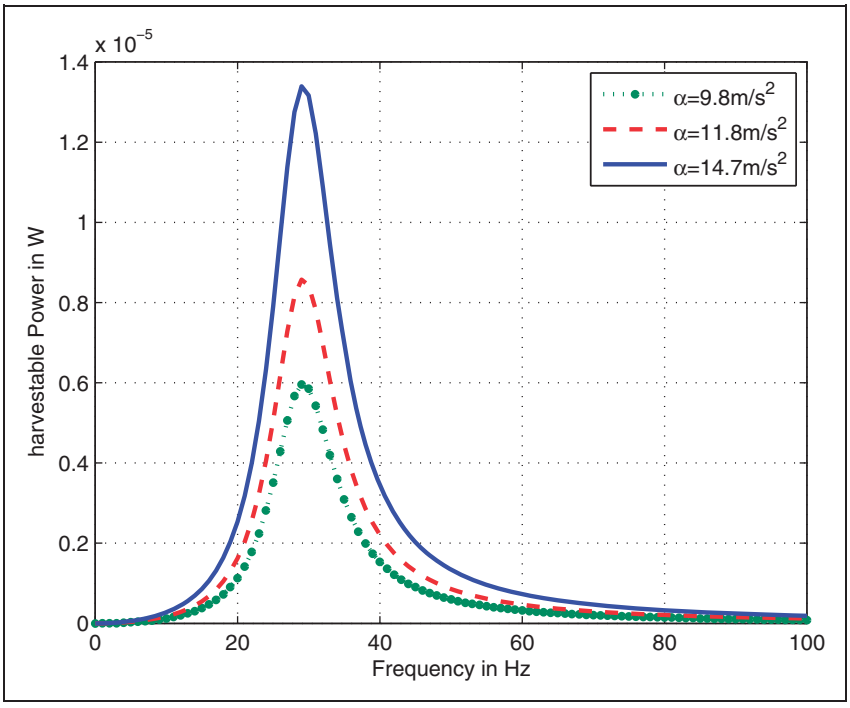

Figure 11. Maximum harvestable power versus frequency.

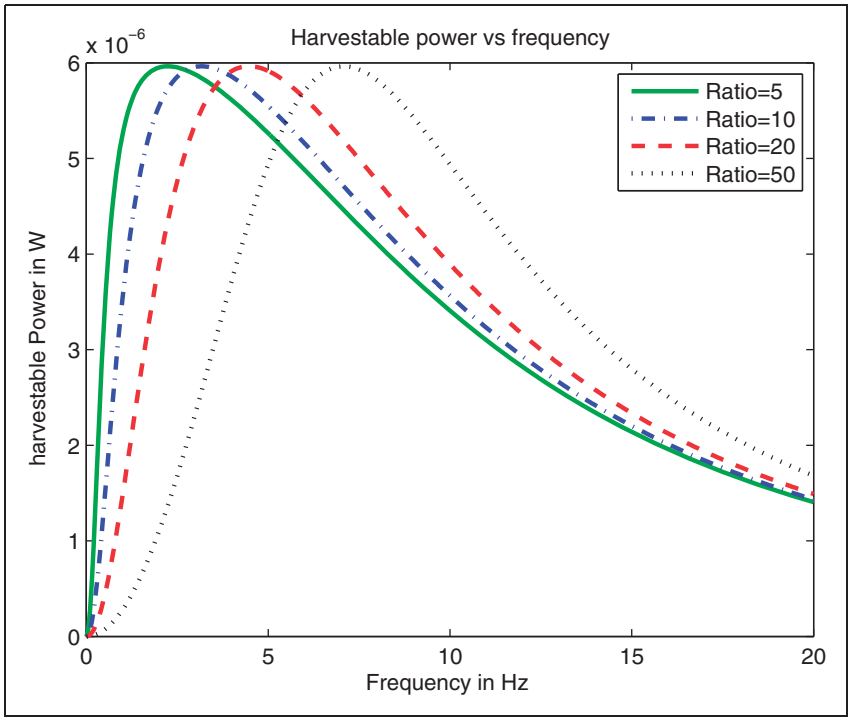

Figure 12. Harvestable power changes by changing the spring stiffness/vibrating mass ratio.

$|Z_{load}| = 100\Omega$. Under the assumption of an energy conservation law, the maximum harvestable energy is plotted based on the following formula (Elvin et al., 2006):

$$P = \frac{\xi_e \omega^2 a^2 M_H^2}{2\left[\omega^2(\xi_e + \xi_m)^2 + (M_H\omega^2 - k_p)^2\right]} \tag{19}$$

where α is the maximum value of the acceleration of the energy harvester (given by $\partial^2 y_2/\partial t_2^2$) and the electrical damping is given by $\xi_e = \left(KN\frac{\partial \Phi}{\partial y_2}\right)^2/Z_{load}$. The harvestable power as a function of the frequency of the oscillating mass in the micro-generator is shown in Figure 11. It can be seen that the larger the maximum acceleration value the larger the harvestable power.

As shown in Figure 11, given the parameters mentioned above, the peak harvestable power is extracted at a frequency of 30 Hz. However this is not a typical natural vibration frequency of a bridge. Usually the maximum acceleration is also a macro parameter that relates to the nature of the vibration and cannot be changed easily. By changing the ratio of the spring stiffness over the harvester mass, we can "shift" the harvester mass vibration frequency attaining peak power at the natural frequency of the bridge. An example of this technique is shown in Figure 12. With a fixed maximum acceleration, by changing the ratio of the spring stiffness/mass, we can shift the power maximizing frequency to a frequency in the 1Hz$\sim$4Hz range, which falls into typical bridge natural frequencies.

6. Conclusions

Structural health monitoring can benefit immensely from the wide use of wireless sensors, due to their inherent characteristics of easy installation with minimal damage to existing structures. However an important concern for wireless sensors is the lifetime of the system, which depends heavily on power supply availability. In order to achieve a lengthy, virtually unlimited lifetime of the system, the sensor nodes should be able to recharge their batteries easily and autonomously. Energy harvesting emerges as a technique that can harvest energy from the surrounding environment. In this paper kinetic energy harvesting from micro-vibrations of the structures on which sensors are attached in order to monitor their structural health has been investigated. After reviewing mathematical models for bridge micro-vibrations, vibration driven electromagnetic harvester solutions have been analyzed and their limitations have been defined. A Maximum-Power-Point-Tracking-based conversion circuit has been introduced that can maximize the conversion coefficient of harvestable kinetic energy to applicable electrical energy.

In the future, we plan to implement our circuit design as a real energy harvesting device and conduct real life experiments to evaluate the applicability and efficiency of our solution to micro-vibration energy harvesting for wireless sensors in the field of SHM.

Acknowledgments

The authors would like to acknowledge their funding body. The opinions expressed in this paper do not necessarily reflect those of the sponsors.

Funding

This work was supported by the European Commission for funding SmartEN (grant number 238726) under the Marie Curie ITN FP7 program.

Notation

m	Mass per unit length of a bridge
c	Damping coefficient of the bridge
E	Young's Modulus of the structure
I	Second moment of area
P	Force to the bridge as a result of a moving load
$\varphi_j(x)$	The j^{th} mode shape function of the bridge
$q_j(t)$	The j^{th} modal displacement
M	Number of modes of significance
$Q_j(\omega)$	the j^{th} modal displacement in the frequency domain
k_p	Stiffness of the spring in the energy harvester
ξ_m	Mechanical damping factor of the energy harvester
ξ_e	Electrical damping factor of the energy harvester.
y_2	Relative displacement of the mass inside the harvester
$y(x,t)$	Displacement of point on the bridge at time t due to vibration
M_H	Mass of the energy harvester
V	Harvester output voltage
C	Piezoelectric capacitance of the energy harvester
Θ	Coefficient of mechanical-electrical coupling
i	The current of the energy harvester (PZT)
Φ	The magnetic flux
K	The number of magnetic stacks
E_{em}	Total harvested electrical energy
F_{ed}	Electrical damping force
E_m^j	Mechanical energy of the j^{th} vibration mode
K_e^2	Electromechanical coefficient
D	Duty cycle of the PWM signal
T_s	Switching frequency of the voltage converter
a	Acceleration of the harvester mass movement.

References

Ali SF and Ramaswamy A (2009) Optimal dynamic inversion based semi-active control of benchmark bridge using MR dampers. *Structural Control and Health Monitoring* 16: 564–585.

Ali SF, Friswell MI and Adhikari S (2011) Analysis of energy harvesters for highway bridges. *Journal of Intelligent Material Systems and Structures* 22: 1929–1935.

ABAQUS (2011) *User Manual V6.11*: ABAQUS Analysis.

Beeby SP, Tudor MJ and White NM (2006) Energy harvesting vibration sources for microsystems applications. *Measurement Science and Technology* 17: 175–195.

Cantero D, Arturo G and O'Brien EJ (2009) Maximum Dynamic stress on bridges traversed by moving loads. *ICE-Bridge Engineering* 162(BE2): 75–85.

Carrella A, Friswell MI, Zotov A, Ewins DJ and Tichonov A (2009) Using nonlinear springs to reduce the whirling of a rotating shaft. *Systems and Signal Processing* 23: 2228–2235.

Casciati F and Rossi R (2007) A power harvester for wireless sensing applications. *Structural Control and Health Monitoring* 14: 649–659.

Casciati S, Faravelli L and Chen Z (2012) Energy harvesting and power management of wireless sensors for structural control applications in civil engineering. *Smart Structures and Systems* 10: 299–312.

Cheng S, Sathe R, Natarajan RD, et al. (2011) A voltage multiplying self-powered AC/DC converter with 0.35 V minimum input voltage for energy harvesting applications. *IEEE Transactions on Power Electronics* 26: 2542–2549.

Dwari S and Parsa L (2009) Low voltage energy harvesting systems using coil inductance of electromagnetic microgenerators. In: *24th IEEE Annual Conference on Applied Power Electronics*, Washington DC, USA, 15–19 February 2009, pp. 1145–1150.

Elvin NG, Lajnef N and Elvin A (2006) Feasibility of structural monitoring with vibration powered sensors. *Smart Materials and Structures* 15: 976–986.

En K, Nakamura M, Yanase T, et al. (2010) Structural health monitoring system applied to rc buildings with smart sensors and wireless network. In *Proceedings of World Conference on Structural Control and Monitoring*, vol. 16, Tokyo, Japan, 12–14 July 2010, pp. 12–14.

Fryba L (1999) *Vibration of Solids and Structures Under Moving Loads*. Thomas Telford.

Han B, Kalis A, et al. (2012) Low cost wireless sensor network for continuous bridge monitoring. In: *6th International Conference on Bridge Maintenance Safety and Management (IABMAS)*, Stresa, Italy, 8–12 July 2012, pp. 96–97.

Han B, Kalis A, et al. (2013) Energy harvesting for sensors in infrastructure monitoring and maintenance. In: *The IABSE Conference on Assessment Upgrading and*

Refurbishment of Infrastructures, Rotterdam, Netherlands, 10–13 May 2013, p. 160.

Halvorsen E (2008) Energy harvesters driven by broadband random vibrations. *Journal of Microelectronic mechanical Systems* 17: 1061–1071.

Jacob B and Labry D (2002) evaluation of the effects of heavy vehicles on bridge fatigue. In: *7th International Symposium on Heavy Vehicle Weights & Dimensions*, Delft, The Netherlands, 16–20 June 2002, pp. 185–194.

Kulkarni S, Koukharenko E, Torah R, et al. (2008) Fabrication and test of integrated micro-scale vibration-based electromagnetic generator. *Sensors and Actuators* 145: 336–342.

Li H, Wekezer J and Kwasniewski L (2008) Dynamic response of a highway bridge subjected to moving vehicles. *Journal of Bridge Engineering* 13: 439–448.

Lynch J and Loh KJ (2006) A summary review of wireless sensors and sensor network for structural health monitoring. *The Shock and Vibration Digest* 38: 91–128.

Massicotte B, Picard A, Ouellet C and Gaumond Y (1994) Strengthening of a long span post tensioned segmental box Girder Bridge. *PCI Journal* 29: 52–65.

McCullagh J, Peterson RL, Galchev T, et al. (2012) Short-term and long-term testing of a vibration harvesting system for bridge health monitoring. In *Proceedings of Power MEMS*, Atlanta, Georgia, USA, 2–5 December 2012, pp. 109–112.

Rahimi A, Zorlu O and Mutharoglu A (2012) Fully self-powered electromagnetic energy harvesting system with highly efficient dual rail output. *IEEE Sensors Journal* 12(6): 2287–2298.

Sazonov E, Li H, Curry D and Pillay P (2009) Self-powered sensors for monitoring of highway bridges. *IEEE Sensor Journal* 9: 1422–1429.

Stancioiu D, Ouyang H, Mottershead JE, et al. (2011) Experimental investigations of a multi-span flexible structure subjected to moving masses. *Journal of Sound and Vibration* 330: 2004–2016.

Sun L (2001) Dynamic displacement response of beam-type structures to moving line loads. *International Journal of Solids and Structures* 38: 8869–8878.

Ulusan H, Gharehbaghi K, Zorlu O, et al. (2012) A self-powered rectifier circuit for low-voltage energy harvesting applications. In: *International Conference on Energy Aware Computing*, Cyprus, 3–5 December 2012, pp. 1–5.

Yang Y, Lina C and Yau J (2004) Extracting bridge frequencies from the dynamic response of a passing vehicle. *Journal of Sound and Vibration* 272: 471–493.